

Regular article

Ab initio MD simulations of a prototype of methyl chloride hydrolysis with explicit consideration of three water molecules: a comparison of MD trajectories with the IRC path*

Misako Aida¹, Hiroshi Yamataka², Michel Dupuis³

¹ Department of Chemistry, Faculty of Science, Hiroshima University, 1-3-1 Kagamiyama, Higashi-Hiroshima 739-8526, Japan

² Institute of Scientific and Industrial Research, Osaka University, Ibaraki, Osaka 567-0047, Japan

³ Pacific Northwest National Laboratory, EMLS/K1-83, Battelle Blvd, Richland, WA 99352, USA

Received: 3 July 1998 / Accepted: 2 September 1998 / Published online: 15 February 1999

Abstract. Ab initio molecular dynamics simulations at the Hartree-Fock/6-31G level of theory are performed on methyl chloride hydrolysis with explicit consideration of one solute and two solvent water molecules at a temperature of 298 K. The reaction involves the formation of a reactant complex and the energy surface to the transition state is found to be simple. Two types of trajectories toward the product are observed. In the first type, the system reaches an intermediate complex (complex-P1) region after two nearly concerted proton transfers involving the attacking water molecule and the solvent water molecules. These trajectories resemble the intrinsic reaction coordinate trajectory. The thermal motion of the atoms leads the system to another intermediate complex (complex-P2) region. A second type of trajectory is found in which the system reaches the complex-P2 region directly after the proton transfers. In both of these forward trajectories, back proton transfers lead the system to a final complex-F region which resembles protonated methanol.

Key words: Ab initio molecular dynamics – Hydrolysis – Intrinsic reaction coordinate – Proton transfer – Solvent effect – Methyl chloride

The attacking species is a water molecule which initially loses a proton to a solvent water molecule with the hydroxide ion formally substituting the chloride ion in methyl chloride. Thus during hydrolysis, bond breaking and bond formation involving both solute and solvent molecules take place. It is essential, therefore, to take the solvent molecules explicitly into consideration in modelling the methyl chloride hydrolysis. Because of this, solvent continuum models [2–4] alone, without explicit account of at least a few solvent molecules, are not expected to be able to describe the mechanism of this type of S_N2 reaction. This is in contrast to type I S_N2 reactions, such as the reaction of a halide anion with methyl halide which has been widely investigated from many aspects and in which bond breaking and bond formation occur only in the solute molecules and the solvent molecules do not participate actively in the reaction except as a bath.

In our previous ab initio molecular orbital (MO) investigations of the methyl chloride hydrolysis [5], we have shown that the reaction energies and the kinetic parameters of the hydrolysis reaction in aqueous solution are well described in the system with 13 water molecules. Moreover, hydrogen-bonded networks of ‘solvent’ molecules are present in the reactant and product complexes and in the transition state (TS) complex as well, which link the attacking water molecule and the chloride atom. A similar network is also present in the smallest cluster with three water molecules. Proton transfers along the hydrolysis reaction path in the 13-water system are also apparent in a 3-water system which we can therefore use as a model system to explore the dynamics of the methyl chloride hydrolysis.

The formal hydrolysis reaction written above does not necessarily represent the actual processes that take place during the reaction in solution where molecular species have varying composition and structure as the reaction proceeds. To understand the active role of the solvent molecules at the molecular level and to explore the evolution of the reaction it should prove very useful

1 Introduction

Hydrolysis is one of the important processes in organic chemistry and in biological systems. The methyl chloride hydrolysis is a type II S_N2 reaction according to Ingold’s classification [1]. The formal chemical formula is:



* Contribution to the Kenichi Fukui Memorial Issue

Correspondence to: M. Aida, H. Yamataka, M. Dupuis

to apply the method of molecular dynamics (MD) [6]. MD is widely used in many fields of chemistry ranging from inorganic materials to biological systems. Most often it is based on the use of empirical interatomic potential functions parametrized to experimental data or to ab initio MO calculations of interaction potentials. It is very laborious and impractical, if not impossible, to construct empirical potential functions to describe bond breaking and bond formation for systems with many atoms. Instead of requiring such empirical potential functions to investigate chemical reactions, the method of direct dynamics can be applied, in which the energy and the forces of the system are computed directly from a quantum mechanical treatment. The direct dynamic method has become increasingly popular, either with semi-empirical [7, 8] or ab initio [9–18] quantum chemical theories. With the rapid advances in computer technology, it is now becoming practical to use ab initio level calculations as the energy and force generators. MD based on ab initio MO methods has also the advantage that computational results can readily be evaluated in terms of the level of theory and the basis set used. In many of these direct dynamic studies [11–15, 18], the MD approach served as a means to probe phase space in search of low energy structures. A few of the studies were concerned with the characterization of chemical reactions.

In this paper we describe the application of the ab initio MD method to the methyl chloride hydrolysis with explicit consideration of three water molecules. This is the first application [19], to the best of our knowledge, to deal with an organic reaction taking explicit account of the solvent molecules by means of MD simulation in which energies and forces are generated by ab initio MO calculations at each time step. The current three-water system is regarded as a prototypical model of the larger cluster and of the reaction in solution. A more complete description of the reaction in aqueous solution would surely require more than three water molecules, yet the present study constitutes a very informative first step in obtaining a detailed description of how the hydrolysis reaction may proceed.

The intrinsic reaction coordinate (IRC) [20, 21] is a minimum energy pathway connecting the TS to the reactants and the products. The calculation of the IRC allows a full characterization of the reaction mechanism. However, the IRC path is obtained under the constraint that the velocity at any given point along the path is zero. At finite temperature, energy flows along the reaction coordinate and among the internal vibrations of the solute and the librations and vibrations of the solvent bath. Thus the finite temperature pathway may differ to a small or large extent from the IRC and may even exhibit molecular processes not observed along the IRC. Such trajectories are in fact observed in the system under consideration.

2 Method

Ab initio MO calculations were performed to obtain the stationary points of the S_N2 reaction of the methyl chloride hydrolysis with an

explicit account of three water molecules at the Hartree-Fock (HF) level of theory with the 6-31G basis set. The reaction involves ionic products so that a single determinant wavefunction represents the system qualitatively correctly. The stationary structures were identified by means of a full analysis of the vibrational frequencies. IRC path calculations were also done. The program packages of HONDO96 [22] and GAUSSIAN 94 [23] were used for these ab initio MO calculations.

Ab initio MD simulations were performed starting at or near the TS structure. Energies and forces were obtained using the same level of theory, namely HF/6-31G. The classical nuclear trajectories were obtained using a fourth-order gear predictor-corrector algorithm [6]. A time step of 0.5 fs was used for the present simulations. The temperature of the system is associated with the classical kinetic energy, and the constant temperature (298 K) algorithm of Berendsen et al. [24] was used. The program package of HONDO96 [22] was used for the ab initio MD calculations.

3 Results and discussion

3.1 Stationary points along the reaction

Figure 1 shows the structures of the stationary points of the S_N2 reaction of the methyl chloride hydrolysis obtained at the HF/6-31G level, which include the initial complex (loosely bound state of CH_3Cl and water cluster), the reactant complex (**complex-R**), the TS, the product complex (**complex-P1**), the second product complex (**complex-P2**) and the final product (**complex-F**). The relative energies of these stationary points are also shown in Fig. 1. Some selected atomic distances are summarized in Table 1 for each stationary point. A calculation of the IRC path shows that TS connects **complex-R** and **complex-P1**.

Complex-P2 features a direct hydrogen bonding interaction between the H1b atom and the Cl ion. This interaction brings additional stability to the system. In **complex-F**, H^+ exists in the form of CH_3OH_2^+ rather than H_3O^+ , consistent with a stronger basicity of CH_3OH than H_2O ; Cl^- is hydrogen-bonded to the proton of CH_3OH_2^+ , the most acidic proton in the system. We were unsuccessful, presumably because of the flatness of the potential energy surface, in determining the TS structure between these stationary points and the IRC paths between them.

The experimental activation enthalpy of the methyl chloride hydrolysis is 26.6 kcal/mol in aqueous solution [25]; it is an exothermic reaction and the reaction enthalpy is estimated to be -6.9 kcal/mol from the data of standard heats of formation in aqueous solution [26]. In the present three-water system, if we regard **complex-R** as the initial state of the reaction, the calculated activation enthalpy (calculated activation energy from Fig. 1 corrected for zero-point vibrational energy) is $+20.1$ kcal/mol, which is in reasonable accord with the experimental activation enthalpy in spite of the limited number of water molecules included in the system and the small basis set used here. In our previous ab initio MO investigation [5], we showed that at least 13 water molecules are necessary to provide a near-quantitative description of the methyl chloride hydrolysis in aqueous solution in terms of the reaction energies and the kinetic parameters. Still the 3-water system exhibits similarities to the 13-water system in the characteristics of the TS,

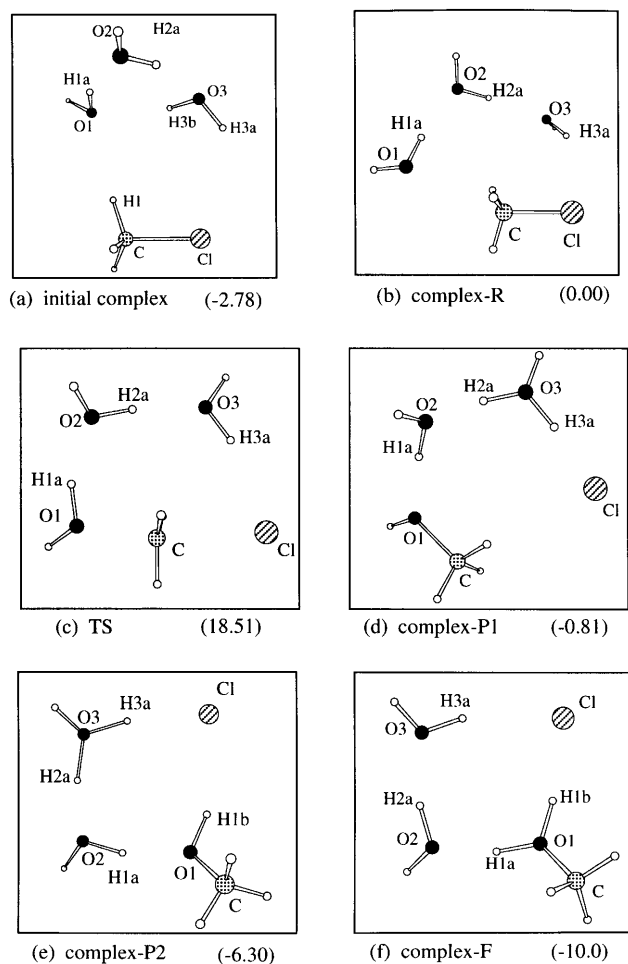


Fig. 1a-f. Structures of the stationary points obtained at the Hartree-Fock 6-31G level. Relative energies (in kcal/mol) are shown in parentheses. Total energies (in hartree) of the stationary points are as follows: **a** -727.058800; **b** -727.054366; **c** -727.024875; **d** -727.055654; **e** -727.064410; **f** -727.070319

and is expected to give a good qualitative description of the reaction processes.

3.2 *Ab initio* MD simulations

Ab initio MD simulations were carried out at 298 K. We performed nine simulations with different initial velocities starting from **TS** (Fig. 1c). In three of the simulation runs, the system was found to evolve in the backward direction, i.e. to move toward the initial state via the **Complex-R** region; in the other runs, the trajectories proceeded in the forward direction toward the product state.

3.2.1 MD trajectory: the backward reaction

One of the simulations corresponding to the backward reaction is shown in Fig. 2. The potential energy change as a function of time is shown in Fig. 2a, and the changes in the atomic distances between C—Cl and C—O1 of the attacking H₂O molecule are shown in

Table 1. Selected atomic distances (in Å) in the stationary points obtained at the Hartree-Fock/6-31G level. See Fig. 1 for the structures and the atomic labels

| | | |
|-----------------|--------|-------|
| Initial complex | C—Cl | 1.880 |
| | O1—H1a | 0.966 |
| | H1a—O2 | 1.789 |
| | O2—H2a | 0.964 |
| | H2a—O3 | 1.826 |
| | O3—H3a | 0.949 |
| | O3—H3b | 0.959 |
| | H3b—O1 | 1.979 |
| | H3a—Cl | 2.857 |
| | H1—O1 | 2.337 |
| Complex-R | C—Cl | 1.898 |
| | C—O1 | 3.000 |
| | O1—H1a | 0.963 |
| | H1a—O2 | 1.800 |
| | O2—H2a | 0.964 |
| | H2a—O3 | 1.786 |
| | O3—H3a | 0.953 |
| TS | C—Cl | 2.518 |
| | C—O1 | 1.867 |
| | O1—H1a | 0.984 |
| | H1a—O2 | 1.624 |
| | O2—H2a | 0.974 |
| | H2a—O3 | 1.712 |
| | O3—H3a | 0.965 |
| Complex-P1 | C—Cl | 2.287 |
| | C—O1 | 1.454 |
| | O1—H1a | 1.636 |
| | H1a—O2 | 0.979 |
| | O2—H2a | 1.445 |
| | H2a—O3 | 1.020 |
| | O3—H3a | 1.061 |
| Complex-P2 | H3a—Cl | 1.756 |
| | C—Cl | 3.804 |
| | C—O1 | 1.433 |
| | O1—H1a | 1.594 |
| | H1a—O2 | 0.989 |
| | O2—H2a | 1.380 |
| | H2a—O3 | 1.048 |
| Complex-F | O3—H3a | 1.026 |
| | H3a—Cl | 1.855 |
| | H1b—Cl | 2.284 |
| | C—Cl | 4.163 |
| | C—O1 | 1.449 |
| | O1—H1a | 1.017 |
| | H1a—O2 | 1.462 |
| O2—H2a | 0.981 | |
| H2a—O3 | 1.638 | |
| O3—H3a | 0.965 | |
| H3a—Cl | 2.268 | |
| H1b—Cl | 1.872 | |
| C—Cl | 3.845 | |

Fig. 2b. The changes in the atomic charge of Cl and in the charge of CH₃ group are shown in Fig. 2c. It is observed that the system stays in the **TS** region during a very short period. The C—Cl bond formation and at the same time the C—O1 bond cleavage are completed around 30 fs (recall this is a 'backward' trajectory). The charges of the Cl and CH₃ fragments vary in concert with the bond length changes for C—Cl and C—O1. A brief plateau is observed in the change of the C—O1 length during the time period of 40–70 fs and it is ascribed to the **complex-R** region, in which the attacking

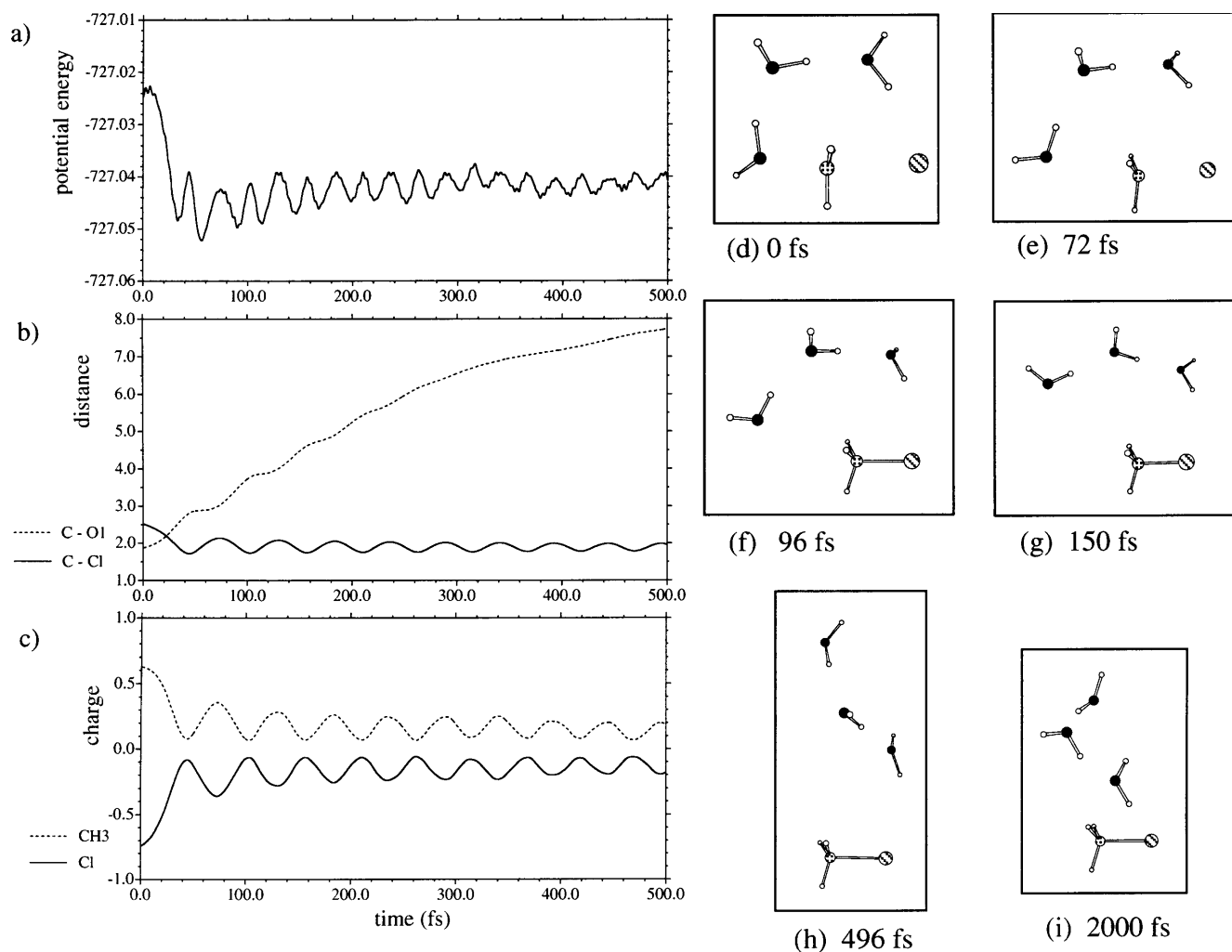


Fig. 2a-i. Trajectory of a backward reaction: **a** potential energy (in hartree); **b** the atomic distances (in Å) between C and Cl and between C and O1; **c** the atomic charge of Cl and the group charge of CH₃ fragment. Snapshot structures at: **d** 0 fs; **e** 72 fs; **f** 96 fs; **g** 150 fs; **h** 496 fs; **i** 2000 fs

H₂O molecule stays near the C atom at a distance of around 3.0 Å. Note that the distance C–O1 is 3.0 Å in **complex-R** (see Fig. 1b and Table 1). After this region, this attacking H₂O moves away toward forming the cyclic H₂O trimer around 1850 fs, and the CH₃Cl molecule remains almost unaffected. Periodic and synchronous changes in the C–Cl length and atomic charges are observed at around 52 fs. This corresponds to a C–Cl bond vibration frequency of around 650 cm⁻¹.¹ The structures of some points along the trajectory are shown in Fig. 2d–i. We can clearly see that the system moves from **TS** via the **complex-R** region toward the initial loosely bound state. We have performed this simulation for 4000 fs and the cyclic H₂O trimer is present all through the trajectory. Overall these

backward trajectories appear simple, little time is spent by the system in the ‘reactive’ part of the trajectory in contrast to the time spent by the system interacting loosely with the solvent trimer.

3.2.2 MD trajectory: a forward reaction from TS – case 1

Figure 3 shows one of the simulations corresponding to the forward reaction in which the system moves toward the product state. The potential energy changes as a function of time are shown in Fig. 3a. The changes in the atomic charges of the oxygen atoms in the three water molecules are shown in Fig. 3b. The changes in the atomic distances between C–Cl and C–O1 of the attacking H₂O molecule are shown in Fig. 3c; those between O1 and H1a and between H1a and O2 in Fig. 3d; those between O2 and H2a and between H2a and O3 in Fig. 3e and those between O3 and H3a and between H3a and Cl in Fig. 3f. From looking at the O–H distance curves, it is very noticeable that the trajectory is made up of three ‘regions’; a ‘**TS** region’ for the first 100 fs, followed by a ‘proton transfer region’ for the next 40 fs and then by a ‘product region’.

In the **TS** region, the first peak in the atomic charge of the attacking O1 atom around 75 fs (Fig. 3b) corre-

¹ The ab initio MO vibrational frequency analysis at the level of HF/6-31G gives 685.5 cm⁻¹ for the C–Cl bond stretching mode for the isolated CH₃Cl.

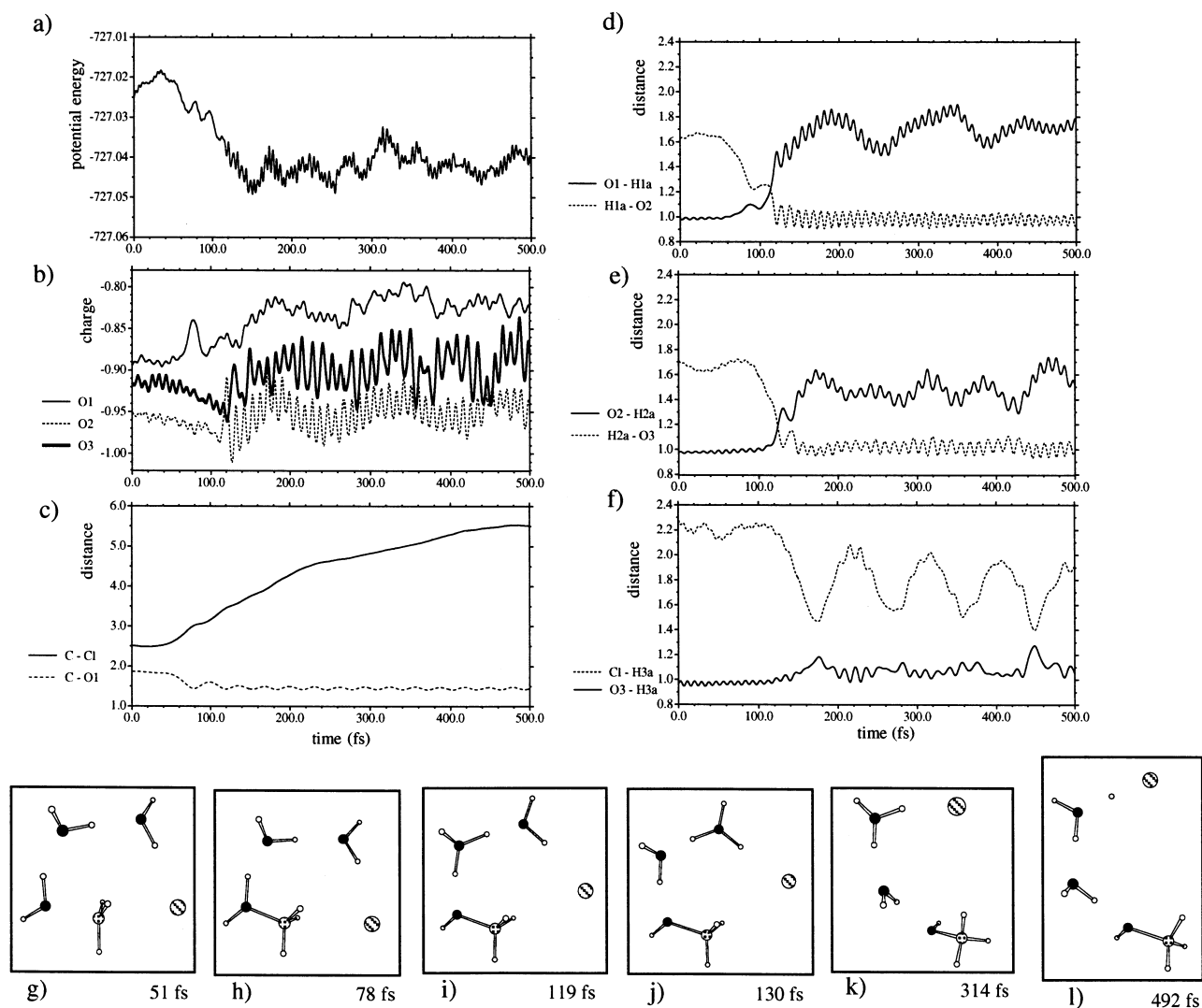


Fig. 3a-l. Trajectory of a forward reaction (case-1) from transition state (TS) toward **complex-P1**: **a** potential energy (in hartree); **b** the atomic charges of O1, O2 and O3 atoms; **c** the atomic distances (in Å) between C and Cl and between C and O1; **d** between O1 and H1a and between H1a and O2; **e** between O2 and H2a and between H2a and O3; **f** between Cl and H3a and between O3 and H3a. Snapshot structures at: **g** 51 fs; **h** 78 fs; **i** 119 fs; **j** 130 fs; **k** 314 fs; **l** 492 fs

sponds to a three bond build-up on the O1 atom as a result of the shortening (formation) of the C—O1 bond in Fig. 3c. From there on the system enters the ‘proton transfer region’ in which a proton relay occurs. The first peak in the atomic charge of the O2 atom around 120 fs (Fig. 3b) corresponds to the formation of H_3O^+ (the first solvent molecule), which coincides with the bond formation of H1a—O2 as shown in Fig. 3d. The first peak in the atomic charge of the O3 atom around 130 fs (Fig. 3b) corresponds to the formation of a H_3O^+ molecule (the second solvent water), which coincides with the bond formation of H2a—O3 as shown in Fig. 3e and indicates that a proton is transferred to this second solvent water. Structures along the trajectory are shown in Fig. 3g–l. After this nearly concerted proton transfer process, the system reaches the **complex-P1** region

around 150 fs. Here, the ‘**complex-P1** region’ means that the optimization of a conformation in this region leads to the **complex-P1**. In the product region, a periodic motion of the proton (H3a atom) is observed between O3 and Cl (Fig. 3f). A snapshot of this region is shown in Fig. 3l. In some configurations (especially around 450 fs), the H3a...Cl distance is very short while H3a...O3 is significantly stretched. Yet it does not appear that the proton transfers fully to the chloride ion.

Thermal motion of the system while in the **complex-P1** region includes an internal rotation of the OH group in CH_3OH about the C—O single bond which allows the proton H1b more favourable interaction with the chloride ion, as suggested in the structure at 314 fs (Fig. 3k). An optimization of the conformation of the trajectory in this phase leads to another product complex (**complex-P2**), which is shown in Fig. 1e. Along the trajectory for up to 500 fs, most of the conformations are within the **complex-P1** region, although a few conformations are within the **complex-P2** region.

We have performed this simulation for a longer time to see how the system would evolve. The whole trajectory of the system up until 2000 fs is shown Fig. 4. The potential energy change as a function of time is shown in

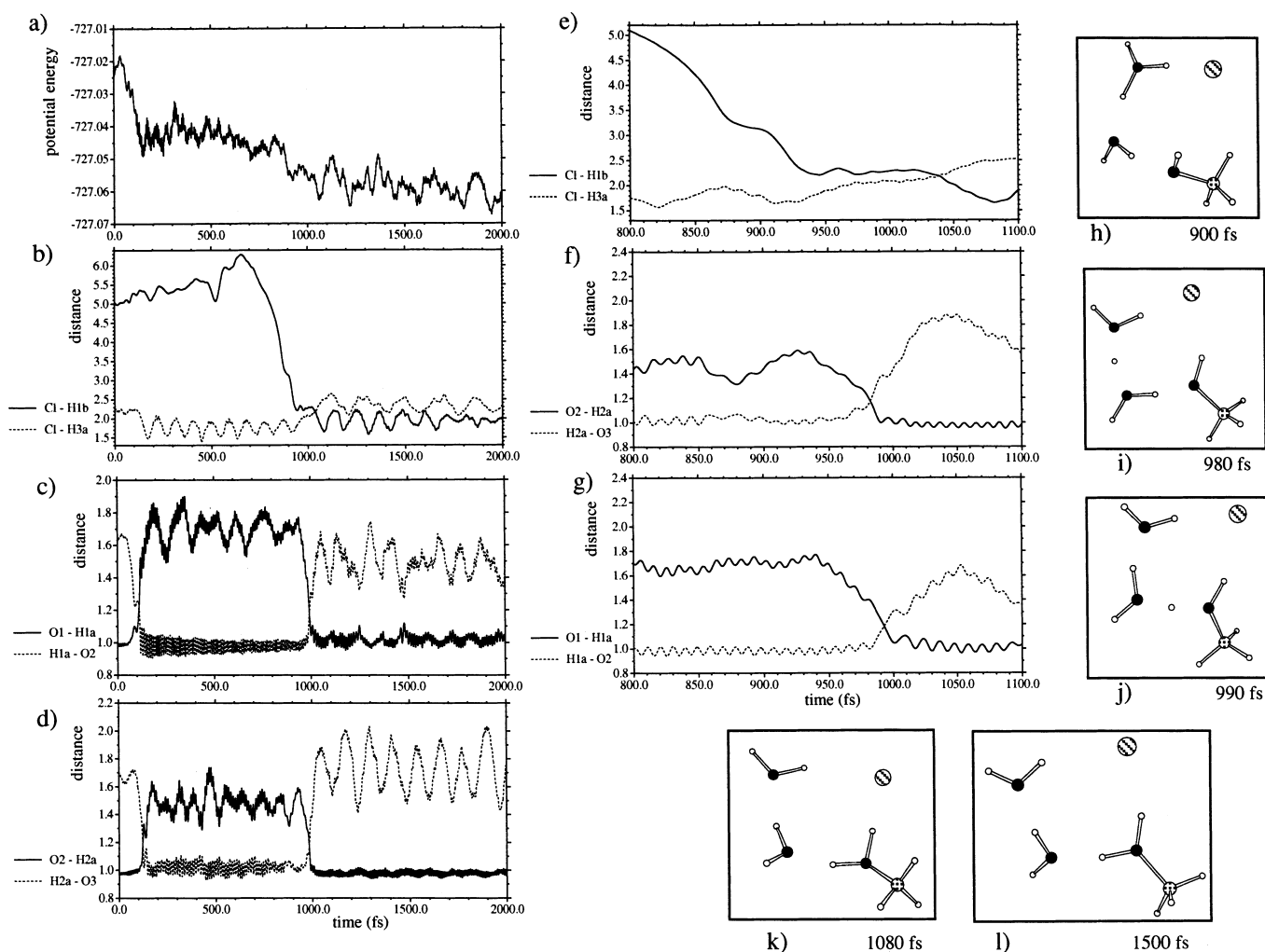


Fig. 4a–l. Trajectory up to 2000 fs of the forward reaction (case-1) shown in Fig. 3: **a** potential energy (in hartree); **b** the atomic distances (in Å) of Cl and H1b and between Cl and H3a; **c** between O1 and H1a and between H1a and O2; **d** between O2 and H2a and between H2a and O3. Trajectory between 800 fs and 1300 fs: **e** the atomic distances (in Å) between Cl and H1b and between Cl and H3a; **f** between O2 and H2a and between H2a and O3; **g** between O1 and H1a and between H1a and O2. Snapshot structures at: **h** 900 fs; **i** 980 fs; **j** 990 fs; **k** 1080 fs; **l** 1500 fs

Fig. 4a; the changes in the atomic distances between Cl and H1b and between Cl and H3a in Fig. 4b; those between O1 and H1a and between H1a and O2 in Fig. 4c and those between O2 and H2a and between H2a and O3 in Fig. 4d. The potential energy of the system becomes lower at around 880 fs (Fig. 4a) which corresponds to the time when, as shown in Fig. 4b, the distance between Cl and H1b becomes shorter, implying that the system is now in the ‘**complex-P2**’ region. Then around 980 fs, another noticeable change is observed: reversed, nearly concerted proton transfers bring the system to the **complex-F** region. The proton H2a, which had transferred to O3 at around 130 fs, goes back to O2 at around 980 fs; the proton H1a, which had transferred to O2 at around 120 fs, goes back to O1 at around 990 fs. The optimization of a conformation in the region after the back proton transfers leads to **complex-F** (Fig. 1f).

To look into the detailed process of the back proton transfers, the bond distance changes of the system between 800 fs and 1100 fs are shown enlarged in Fig. 4e–g. It can be seen that the distance between Cl and H1b becomes shorter at around 930 fs, when the back proton transfer has not yet occurred; during an interval of about 30 fs, the system is in the **complex-P2** region. After the nearly concerted proton transfers, the system changes to the **complex-F** region. The structures of some points along the trajectory are shown in Fig. 4h–l. The final product (**complex-F**, Fig. 1f) looks as if it were a direct adduct of H₂O to the CH₃⁺ moiety. It should be stressed, however, that **complex-F** cannot be formed directly from TS.

3.2.3 MD trajectory: a forward reaction from TS – case 2

Figure 5 shows a different type of trajectory in which the system moves toward the product state. The potential energy change as a function of time is shown in Fig. 5a; the changes in the atomic charges of the oxygen atoms in three water molecules are shown in Fig. 5b; the changes in the atomic distances between C–Cl and C–O1 of the attacking H₂O molecule are shown in Fig. 5c; those between O1 and H1a and between H1a and O2 in Fig. 5d;

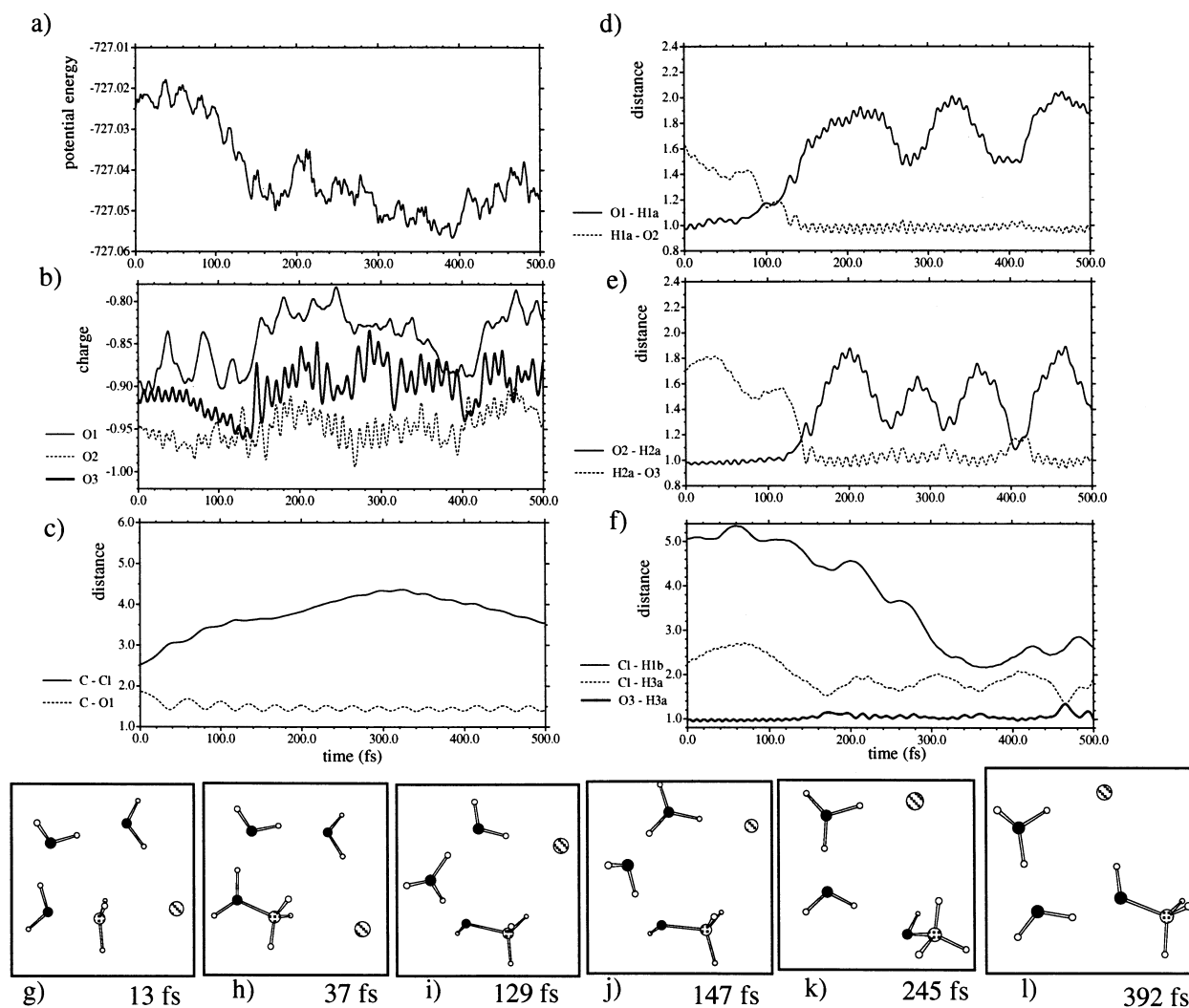


Fig. 5a–l. Trajectory of a forward reaction (case-2): **a** potential energy (in hartree); **b** the atomic charges of O1, O2 and O3 atoms; **c** the atomic distances (in Å) between C and Cl and between C and O1; **d** between O1 and H1a and between H1a and O2; **e** between O2 and H2a and between H2a and O3; **f** between Cl and H1b, between Cl and H3a and between O3 and H3a. Snapshot structures at: **g** 13 fs; **h** 37 fs; **i** 129 fs; **j** 147 fs; **k** 245 fs; **l** 392 fs

those between O2 and H2a and between H2a and O3 in Fig. 5e and those between O3 and H3a, Cl and H3a and Cl and H1b in Fig. 5f. In this simulation, once the C–O1 bond formation is completed around 35 fs, a rather large vibration of the attacking water molecule is observed until around 120 fs. Note the specific peaks in the atomic charge variation of the O1 atom at around 37 fs and 81 fs (Fig. 5b). These peaks correspond to the formation of the protonated methanol. Then, the nearly concerted proton transfer begins to occur: a proton (H1a) moves to the second water at around 130 fs, and next, a proton (H2a) moves to the third water at around 145 fs. The structures of some points along the trajectory are shown in Fig. 5g–l. We have performed the optimization procedures on some points along the trajectory, and confirmed that the system is in the **complex-P1** region before 120 fs although the system is in the **complex-P2** region after 120 fs.

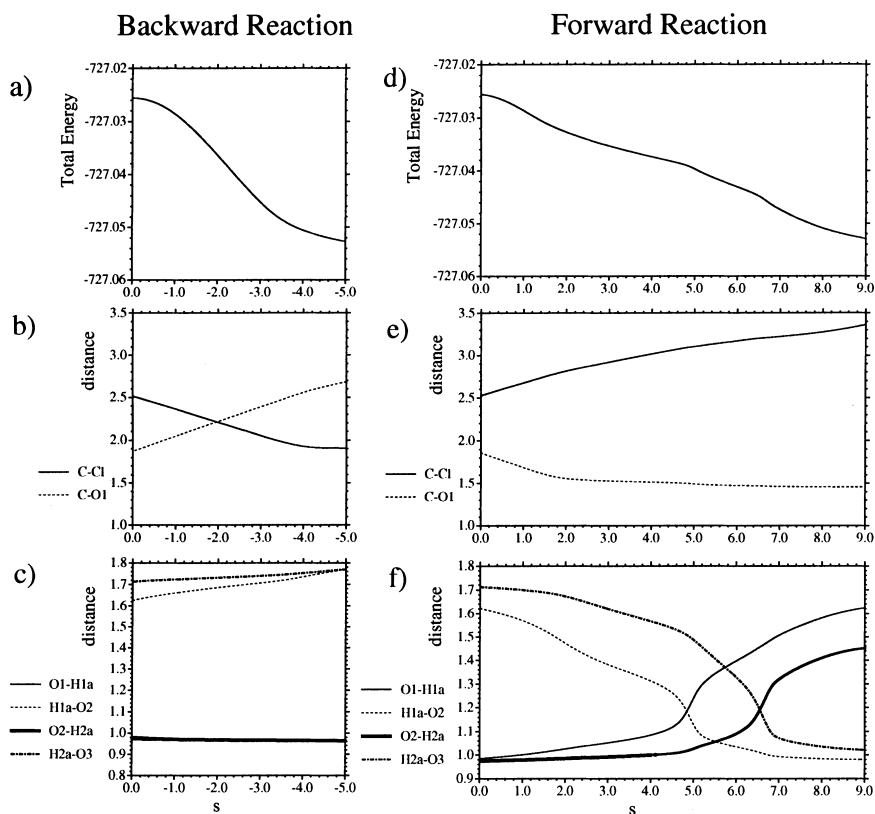
Here, the ‘**complex-P2** region’ means that the optimization of a conformation in this region leads to the **complex-P2**. It should be noted that the period of the proton transfers is in the **complex-P2** region. The system moves toward the **complex-P2** region *without going through the complex-P1* region. This is because the H1b atom faces the Cl atom at a rather early stage in the transition state region. This tendency is brought about by thermal motions created by random initial velocities.

We have performed this simulation until 2000 fs (data not shown). The system stays in the **complex-P2** region until around 950 fs, when the nearly concerted back proton transfers begin to occur and bring the system to the **complex-F** region. The proton H2a, which has transferred to O3 around 130 fs, is now back to O2 around 970 fs; the proton H1a, which has transferred to O2 around 100 fs, is now back to O1 at around 990 fs. This process is very similar to that found in another simulation described in the previous section.

3.3 Comparison of MD trajectories with IRC path

The approach followed in the ab initio MD simulation starting from TS is essentially equivalent to calculating

Fig. 6a-f. Intrinsic reaction coordinate path obtained at HF/6-31G. Backward reaction from TS ($s=0$) toward **complex-R**: **a** total energy (in hartree); **b** the atomic distance changes (in Å) between C and Cl and between C and O1; **c** between O1 and H1a, between H1a and O2, between O2 and H2a and between H2a and O3. Forward reaction from TS ($s=0$) toward **complex-P1**: **d** total energy (in hartree); **e** the atomic distance changes (in Å) between C and Cl and between C and O1; **f** between O1 and H1a, between H1a and O2, between O2 and H2a and between H2a and O3.



reaction path trajectories at finite temperature, in contrast to the IRC path [20, 21] at 0 K. In this section, we contrast the MD trajectories and the IRC path in the present system.

The IRC path calculations showed that **TS** connects **complex-R** and **complex-P1**. The variations of the energy and the selected atomic distances along the IRC path for each backward reaction and forward reaction are illustrated in Fig. 6. The IRC path is defined starting from the TS structure. From a quantum chemical description, the TS structure would usually be ascribed as the region of phase space where bond formation and bond breaking take place. In the present S_N2 reaction, the O1-C bond formation and the C-Cl bond breaking correspond to those major bonding changes at the TS. Starting from $s=0$ (**TS**) toward the reactant (negative s), the C-Cl length becomes shorter (Fig. 6b) indicating the formation of CH_3Cl ; it is almost unchanged after around $s=-4$. At $s=-5.0$, the system is close to **complex-R**.

According to the MD trajectories corresponding to the backward reaction from **TS**, the system reaches the reactant complex around 50 fs (Fig. 2). The energy profile and the atomic distance evolutions along the MD trajectory at 298 K until around 50 fs in Fig. 2a, b compare with those along the IRC path in Fig. 6a, b. This is probably because the potential energy surface along this backward reaction is not intricate and the process of the reaction does not depend much on the temperature of the system. The MD trajectory indicates that the essential process of this backward reaction from **TS** to **complex-R** is completed in less than

50 fs, soon after the TS. After the reactant complex region, the formation of the water trimer proceeds slowly and the system moves toward the loosely bound complex of CH_3Cl with the water trimer. The kinetic energy/temperature is what allows the system to evolve in and out of the shallow well of the entrance complex.

Along the IRC path which starts from **TS** ($s=0$) and goes to **complex-P1** (the forward reaction: positive s), the C-O1 length becomes short (Fig. 6e) indicating the formation of CH_3OH_2 ; the C-O1 length is almost unchanged after around $s=2$. Then, the first proton transfer occurs at $s=4.8$ from the attacking water to the first solvent molecule, followed by the second proton transfer which occurs at $s=6.5$ from the first solvent water to the second solvent water (Fig. 6f). At $s=9.0$, the system is close to **complex-P1**. The IRC path toward **complex-P1** clearly shows the existence of successive proton transfers involving the attacking water molecule and the solvent water molecules after the TS on the way to the formation of the product complex. In the present ab initio MD simulations at 298 K, as is shown in Fig. 3, the system stays in the 'TS region' around 50 fs in which no apparent change occurs. Then the O1-C bond formation and the C-Cl bond breaking start to occur, followed by the nearly concerted proton transfers at around 120 fs. The energy profile and the atomic distance evolutions along the MD trajectory at 298 K from 50 fs until 120 fs in Fig. 3a, c-e compare with those along the IRC path in Fig. 6d-f. The concertedness of the proton transfers observed in the MD trajectories is much less apparent in the IRC path.

In the MD trajectories, it should be noted that the ‘TS region’ is a region in which the system resides for some time with bonds ‘half-broken and half-formed’ before it reaches a region of ‘real transition’ marked by the nearly concerted proton transfers which take place over a very short period of time, after which the system enters the product region. We have performed several simulations which proceed toward the product state, and found the same characteristics of the ‘TS region’ and the ‘proton transfer region’ in all the simulations which moved toward **complex-P1**. No such ‘TS region’ was observed in any of the ‘backward’ trajectories. Such a finding is a reflection of the different character of the potential energy surface on the two sides of the TS. The energy surface is much less intricate in the reactant-side region than in the product-side region which has more numerous hydrogen-bonding interactions. The energy released along the reaction mode gets transferred into the transverse modes, in particular the ‘cluster’ proton transfer modes. A more complete analysis of the vibrational quantum dynamics of the system along the reaction path using the reaction path Hamiltonian for example [27] would be needed to gain insight on the appearance of these reaction stages.

As was described in the previous section, we have observed other trajectories which are different from the IRC path, namely the reaction pathway from **TS** to **complex-P2**. In such a trajectory (Fig. 5), the **Ol—C** bond formation and the **C—Cl** bond breaking start to occur soon after **TS**; however, the period of a rather large vibration of the attacking water molecule lasts until around 130 fs. During the period, the Cl atom moves close to the H_{1b} atom and then the nearly concerted proton transfers lead the system toward the **complex-P2** region, without passing the **complex-P1** region.

3.4 MD trajectory crossing TS

In general, a chemical reaction is a very rare event, since a reaction channel is very narrow and furthermore excess energy would be needed to climb up a TS. It would be necessary to perform long MD simulations with a great many different initial velocities to represent a chemical reaction, if they start from arbitrary points on the potential surface. This is the reason why we have performed the simulations starting from the TS structure in the present investigation as described in the previous sections. Starting from the TS structure, the system would easily follow the reaction channels toward the reactant region and also toward the product region. However, there might be other reaction pathways in which the system would not pass through the TS structure. MD simulations starting from non-TS structure would give information which cannot be given by those starting from TS.

We have performed such MD simulations, starting from the structure which corresponds to the tenth step on the trajectory of the backward reaction (Fig. 2) with different initial velocities. We have performed seven simulations and have found three of them evolving toward the reactant region and four of them evolving toward the product region; their evolutions are similar

to those described in the previous sections for the corresponding trajectories starting from **TS**. Figure 7 shows one of the simulations which evolves toward the product region. Here note that the point of time = 0 does not correspond to the TS. The potential energy change as a function of time is shown in Fig. 7a; the changes in the atomic distances between **C—Cl** and **C—Ol** are shown in Fig. 7b. It should be noted that the **C—Cl** bond length is 2.518 Å and **C—Ol** bond length is 1.867 Å at **TS**, (see Table 1). The bond length changes in this trajectory (Fig. 7b) show that the reaction does not pass through the TS, which is determined in the framework of ab initio MO theory. The MD simulations here indicate that the reaction might proceed not through the saddle point but through a region around it at finite temperature.

4 Conclusions

The present ab initio MD simulations exhibit dynamic features of the S_N2 reaction of methyl chloride with three water molecules, which can be regarded as a prototype of the methyl chloride hydrolysis in aqueous solution. The backward reaction and the forward

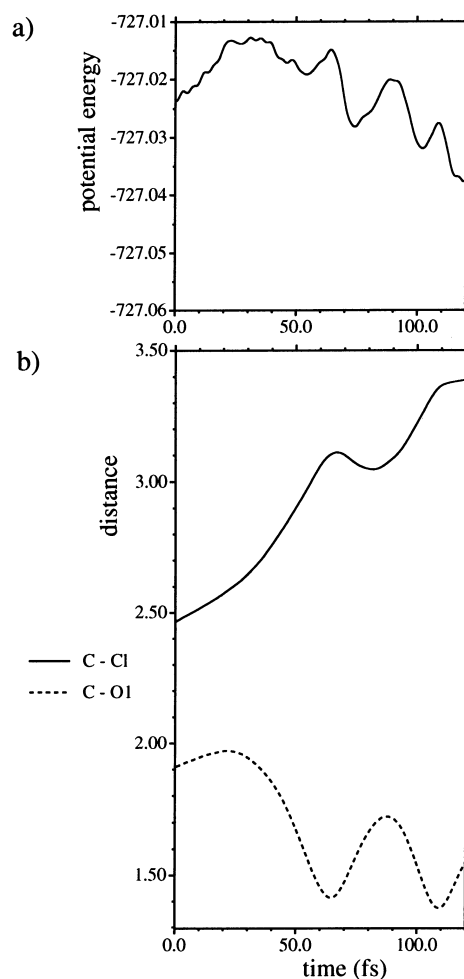


Fig. 7a, b. Trajectory of a forward reaction starting from a non-TS structure: **a** potential energy (in hartree); **b** the atomic distances (in Å) between C and Cl and between C and Ol

reaction show the different features. The backward reaction proceeds very quickly; the attacking water molecule goes away from the methyl chloride soon after the TS; and the system passes the reactant complex (**complex-R**) region around 50 fs and then the water trimer is formed around 2000 fs. In the forward reaction, the attacking water molecule keeps two hydrogen atoms in the transition region and this period lasts around 100 fs. And then, the nearly concerted proton transfers occur and an intermediate complex (**complex-P1** region) is formed around 150 fs. With further thermal motions, the system reaches the final complex region after 1000 fs. The trajectories from the **complex-R** region through the **TS** region to the **complex-P1** region are those which trace the IRC path. Other trajectories which are different from the IRC path are observed for the forward reaction, in which the system moves to another intermediate complex (**complex-P2**) region after the nearly concerted proton transfers. The IRC path is not the only path along which the reaction proceeds at finite temperature. In either pathway, the nearly concerted back proton transfers lead the system to the same final product. The ab initio MD simulation is a powerful technique to explore the reaction processes at finite temperature.

The observation of the proton transfers in the forward reaction clearly indicates that it is essential to take at least a few solvent molecules explicitly into consideration as part of the quantum mechanically treated system to describe the methyl chloride hydrolysis, not just as creating a reaction field, but rather as actively participating in the reaction. This finding is likely to have significance with regard to modelling of reactions in solutions using continuum dielectric models and quantum mechanics/molecular mechanics models, neither of these approaches having the capability to describe the intricate processes observed here, unless some actively participating solvent molecules are included in the quantum part. Many more than two solvent water molecules would be needed to describe realistically the reaction in aqueous solution, yet the present work already provides much insight into the hydrolysis reaction at the molecular level.

Acknowledgements. The numerical calculations were carried out on the IBM/RS6000 Powerstations at the National Cancer Center Research Institute and at Osaka University, as well as on the SP2 at the computer center of the Institute for Molecular Science. The Pacific Northwest National Laboratory is a multiprogramme national laboratory operated for the U.S. Department of Energy by Battelle Memorial Institute under Contract DE-AC06-76RLO 1830.

References

1. Ingold K (1969) Structure and mechanism in organic chemistry, 2nd edn. Cornell University Press, London
2. Wong MW, Frisch MJ, Wiberg KB (1991) *J Am Chem Soc*, 113:4776
3. Miertus S, Scrocco E, Tomasi J (1981) *Chem Phys* 55:117
4. Klamt A, Schürmann G (1993) *J Chem Soc Perkin Trans* 2:799
5. Yamataka H, Aida M (1998) *Chem Phys Lett* 289:105
6. Allen MP, Tildesley DJ (1987) *Computer simulations of liquids*. Oxford University Press, Oxford
7. Truhlar DG (1995) In: Heidrich D (ed) *The reaction path in chemistry: Current approaches and perspectives*. Kluwer, Dordrecht, The Netherlands, p 229
8. Peslherbe GH, Hase WL (1996) *J Chem Phys* 104:7882
9. Car R, Parrinello M (1985) *Phys Rev Lett* 55:2471
10. Greer JC, Ahlrichs R, Hertel IV (1991) *Z Phys D* 18:413
11. Hartke B, Carter EA (1992) *Chem Phys Lett* 189:358
12. Maluendes SA, Dupuis M (1992) *Int J Quantum Chem* 42:1327
13. Uggerud E, Helgaker T (1992) *J Am Chem Soc* 114:4265
14. Jellinek J, Bonacic-Koutecky V, Fantucci P, Wiechert M (1994) *J Chem Phys* 101:10092
15. Reichardt D, Bonacic-Koutecky V, Fantucci P, Jellinek J (1997) *Chem Phys Lett* 279:129
16. Tunon I, Martins-Costa MTC, Millot C, Ruiz-Lopez MF (1997) *J Chem Phys* 106:3633
17. Steckler R, Thurman GM, Watts JD, Bartlett RJ (1997) *J Chem Phys* 106:3926
18. Wei D, Salahub DR (1997) *J Chem Phys* 106:6086
19. Preliminary report Aida M, Yamataka H, Dupuis M (1998) *Chem Phys Lett* 292:474
20. Fukui K, (1970) *J Phys Chem* 74:4161
21. Ishida K, Morokuma K, Komornicki A (1977) *J Chem Phys* 66:2153
22. Dupuis M, Marquez A, Davidson ER (1996) HONDO 96, available from the Quantum Chemistry Program Exchange, Indiana University, Ind
23. Frisch MJ, Trucks GW, Schlegel HB, Gill PM W, Johnson BG, Robb MA, Cheeseman JR, Keith TA, Petersson GA, Montgomery JA, Raghavachari K, Al-Laham MA, Zakrzewski VG, Ortiz JV, Foresman JB, Cioslowski J, Stefanov BB, Nanayakkara A, Challacombe M, Peng CY, Ayala PY, Chen W, Wong MW, Andress JL, Replogle ES, Gomperts R, Martin RL, Fox DJ, Binkley JS, Defrees DJ, Baker J, Stewart JP, Head-Gordon M, Gonzalez C, Pople JA (1995) GAUSSIAN 94, Revision C.2. Gaussian Inc., Pittsburgh, PA
24. Berendsen HJC, Postma JPM, van Gunsteren WF, DiNola A, Haak JR (1984) *J Chem Phys* 81:3684
25. Abraham MH, McLennan DJ (1977) *J Chem Soc Perkin Trans* 2:873
26. Lias SG, Bartmess JE, Holmes JL, Levin RD, Mallard GW (1988) *J Phys Chem Ref Data Suppl* 17:1
27. Miller WH, Handy NC, Adams JE (1980) *J Chem Phys* 72:99